AIAA JOURNAL
Vol. 43, No. 8, August 2005

Real-Time Structural Damage Monitoring by Input Error Function

B. H. Koh,* P. Dharap,† and S. Nagarajaiah‡
Rice University, Houston, Texas 77005
and
M. Q. Phan§
Dartmouth College, Hanover, New Hampshire 03755-8000

A newly developed structural damage monitoring technique is presented. The study focuses on capturing the initiation of multiple damages as they occur in a structure, which is similar to the concept of the fault detection filter. Previously, it has been shown that modified interaction matrix formulation provides a series of input error functions that generate a nonzero residual signal when the system experiences erroneous inputs. Error functions for each individual structural member are developed from the analogy between actuator failure and damage-induced residual force. When each individual error function is monitored, multiple damages as they occur in a structure can be simultaneously detected and isolated. Because the technique does not require frequency-domain measurements, it is readily applicable to online monitoring systems. This real-time technique also accommodates nonlinear breathing cracks and works for any type of excitation. A numerical simulation using a spring–mass system and truss structure successfully demonstrates the proposed method.

I. Introduction

BECAUSE of unprecedented demand on the precision and reliability, real-time damage monitoring has become a critical issue in some of the intelligent structures. Good examples include aerospace structures, rotating machinery, and smart structures that are already in operation or properly conditioned by feedback control. The purpose of real-time monitoring is to take immediate actions to alleviate the consequence of damage as it occurs in the structure. The goal of this study is to develop a new algorithm that captures the onset of incipient structural degradation in real time. Here, real time means that structural properties are changing or degrading as a function of time due to unknown damage. Strictly, real-time damage monitoring is different from a traditional modal-based diagnostic method, which can be categorized as an off-line, intermittent inspection. A modal-based damage detection method employs a quantitative examination of frequency-domain measurements (natural frequency, mode shape, frequency-response function, etc.) from the structure.[1−4] Therefore, there exists a significant time delay due to user interaction between the initiation of damage and its diagnosis. One of the well-known modal-based damage detection methods exploits the concept of optimal matrix updating along with minimum-rank perturbation theory.[5] This approach requires natural frequencies and mode shapes information from a modal testing. Some of the other damage detection algorithms use correlations between the measured frequency-response function (FRF) of the damaged structure and the analytic model of the healthy structure.[6] Whether it is modal frequency or FRF measurement, the nature of the modal-based technique is intrinsically off-line because extracting those damage-sensitive structural properties requires data condensation and domain transition. Although there have been recursive estimation techniques for real-time modal parameter identification,[7] extracting modal properties from time histories is generally considered as an off-line process. Therefore, it is difficult to capture the moment of damage initiation by solely observing the frequency-domain measurements.

On the other hand, time-domain approaches, including the proposed method in this paper, directly assess the condition of structure from the measured time histories.[8−10] This signal-based diagnosis procedure is well developed in the field of fault detection in a control system.[11−13] Most of the well-known time-domain fault detection methods use a model-based redundancy strategy.[14] The simplest way of diagnosing fault in a system is equipping the system with physical redundancy such as triplicate sensors so that a failed sensor or actuator can be detected by a simple voting logic. Analytical redundancy (AR) is a mathematical alternative for physical redundancy.[15] The basic idea of the AR approach is that the observed nonzero error signals generated by differences between response from the analytical model and measured response can be an indication of a fault in a system. Thus, it is important to generate an error signal when the dynamic property of the system has been changed by unknown faults. Also, the generated error signal should be systematically decoupled so that each error signal matches one-to-one with the individual system component that is being examined. The ultimate goal of the AR-based fault diagnosis method is detecting and isolating unknown faults in system components so that adaptive controller can compensate those errors to stabilize the system in real time. Because the AR-based method necessitates a mathematical model of the system, it belongs with model-dependent methods. Typically, system identification techniques are employed to generate this analytical model.

Although a lot of studies have been conducted on the fault detection and isolation problem in control systems, surprisingly there is a very limited number of papers on structural damage detection using AR strategies. Kranock[16] developed a model-based damage detection filter to identify real-time damage that occurred in a truss structure. The technique exploits the concept of state-space observer and parameterizes the feedback gain for damage localization. In the experiment, real-time stiffness damage is inflicted by a melting plastic device placed on one of the truss members. Seibold and Weinert[17] presented a damage detection algorithm for a rotor dynamic system using a Kalman filter bank; each filter represents specific damage

Received 15 October 2004; revision received 24 January 2005; accepted for publication 24 January 2005.

*Postdoctoral Research Associate, Department of Civil and Environmental Engineering; currently Postdoctoral Research Associate, Department of Civil Engineering, Washington University, St. Louis, MO 63130-4899. Member AIAA.

†Graduate Student, Department of Civil and Environmental Engineering.

‡Associate Professor, Departments of Civil and Environmental Engineering and Mechanical Engineering and Material Science. Member AIAA.

§Associate Professor, Thayer School of Engineering. Member AIAA.

scenario and the crack is localized by examining the hypothesis of innovation from the filter. More recently, Demetriou and Hou,[18] investigated a real-time method using a wavelet and neural network to detect abrupt changes in stiffness of a simple spring–mass system.

Another significant advantage of signal-based monitoring technique over the modal-based methods is the capability of accommodating a nonlinear damage mechanism such as a breathing crack. Most of the frequency-domain methods focused on identifying open-crack damage model, which assumes that the dynamic stiffness of crack remains the same during the vibration. In other words, it is presumed that the crack surfaces do not contact each other even in a compression mode. However, the stiffness of a structural member having a fatigue surface crack will change alternately as the structure vibrates between elongation and compression modes. Consequently, the natural frequency of a structure having a breathing crack is different from the one with a fully opened crack.[19] There are several reports indicating that crack-closing or crack-breathing behavior of a surface crack tends to diminish the amount of modal frequency shift. Cheng et al.[20] demonstrated that the open-crack assumption might underestimate the true severity of a fatigue crack in modal-based methods. Chondros et al.[21] also point out that the open-crack model may provide a misleading conclusion about the amount of frequency drop in an aluminum beam when a fatigue breathing crack is considered. In the real world, the breathing crack is considered as a more practical example of structural defect; loosened bolts, couplings, and press-fitted and riveted joints exhibit similar bilinear behaviors of a fatigue breathing crack.[22]

In this study, the interaction matrix is used to derive a series of decoupled output error signals for structural damage detection. The interaction matrix, first proposed by Phan et al.,[23] provides an intrinsic equivalence of an input–output model with a state-space model. The concept of an interaction matrix has been applied to state estimation,[24] system and disturbance identification,[25] vibration suppression, disturbance rejection, tracking by predictive control,[26,27] and actuator failure detection.[28] In the study of identifying the system of disturbance-free dynamics, the interaction matrix explicitly eliminates the dependence of the state variables so that unknown disturbance inputs can be separated from the system and its input–output model. Moreover, imposing the condition of interaction matrix further decouples the intertwined multi-input/multi-output system so that effects of erroneous input can be independently separated.[28] Because the influence of each input can be individually examined regardless of the condition of other inputs, this technique can be readily applied to detect actuator failure given the analytical model of the system. If the fault of the input to the system is exclusively identifiable, the same idea extends to the detection structural damage. Without loss of generality, the effect of mass or stiffness damage can be simulated to an input failure with equivalently compensated error force. This paper aims to identify structural damage by exploiting the analogy between residual force due to stiffness change and input error. Specifically, a model-based, real-time structural damage monitoring method will be investigated that employs decoupled input–output equations using the modified formulation of interaction matrix. When stiffness damage occurs to one of the structural members, nonzero error signals are generated as if the virtual actuator of the corresponding member has failed. Once coefficients of the error function are determined from the state-space model of a healthy structure, the residual is generated by a simple linear equation. Thus, the monitoring process itself is computationally efficient and does not occupy large memory. Also, a bilinear breathing crack is considered as a realistic damage model to emphasize the advantage of the method over other off-line modal-based approaches. Through the paper, the theoretical background is explained, and the effectiveness of the method is illustrated by numerical examples such as a spring–mass system and three-dimensional truss structure.

II. Theoretical Background

A. Equivalence of Stiffness Damage and Input Error

In this section, we develop a theoretical connection between stiffness damage and actuator failure in a dynamic system. Here, a second-order dynamic system is given in the physical coordinate $\boldsymbol{q}(t)$, where the external input to the system is denoted as $\boldsymbol{u}(t)$:

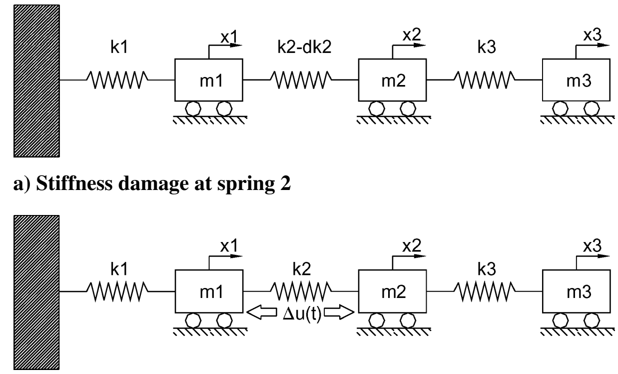

a) Stiffness damage at spring 2

b) Equivalent input force error $\Delta \boldsymbol{u}(t)$

Fig. 1 Schematic of three-DOF spring–mass system with stiffness damage in spring 2 and equivalent input force error.

$$M\ddot{\boldsymbol{q}}(t) + \Theta\dot{\boldsymbol{q}}(t) + K\boldsymbol{q}(t) = B_f\boldsymbol{u}(t) \tag{1}$$

M, Θ, and K are mass, damping, and stiffness matrices, respectively. The matrix B_f is the input influence matrix that connects each input to the corresponding degree of freedom. The structural damage can be expressed as a perturbation of stiffness matrix (ΔK) from the undamaged stiffness matrix K:

$$M\ddot{\boldsymbol{q}}(t) + \Theta\dot{\boldsymbol{q}}(t) + (K - \Delta K)\boldsymbol{q}(t) = B_f\boldsymbol{u}(t) \tag{2}$$

Then, the equivalence of stiffness damage and input error can be justified via $\Delta\boldsymbol{u}(t) = \Delta K\boldsymbol{q}(t)$, or

$$M\ddot{\boldsymbol{q}}(t) + \Theta\dot{\boldsymbol{q}}(t) + K\boldsymbol{q}(t) = B_f\boldsymbol{u}(t) + \Delta\boldsymbol{u}(t) \tag{3}$$

To illustrate the equivalence of stiffness damage and input error, the three-degree-of-freedom (DOF) spring–mass system is considered (Fig. 1). Stiffness damage ΔK in spring 2 can be replaced by internal input forces $\Delta\boldsymbol{u}(t)$ between masses 1 and 2, as shown in Fig. 1. Each mass of the system is excited by random noise input, and the corresponding displacement measurements are collected. Figure 2 shows the response of the system experiencing the stiffness damage, or equivalently input force error. It is assumed that stiffness of the spring 1, k_1, is intermittently changed after 2 s and fully recovered after 4 s. Again, the same stiffness variation of the spring 1 occurs after 6 s. Also, springs 2 and 3 experience stiffness changes for 3 s at different time instants. Although the starting time of stiffness change is noticeable from the response, the profile of the individual stiffness variations is not obvious. Because each output is intertwined with the influences of all other inputs, the information regarding the time and location of the stiffness change is hidden. Thus, an algorithm is needed to decouple the influence of stiffness variation from the overall outputs of the system so that the individual damage can be isolated regardless of the other states. We will find this algorithm from the analogy between stiffness damages and input errors. In the following section, the formulation of the input error function is introduced. This error function is developed by imposing the necessary condition of interaction matrix in a state-space framework, which will eliminate the influence of other input errors except for the one being examined.

B. Condition of Interaction Matrix and Input Error Function

Previously, the input error function for the actuator failure detection problem has been developed.[28] It will be explained here again for completeness. Because the input error function is developed in a state-space framework, the second-order equation (1) should be expressed in first-order form. Consider an nth-order, r-input, m-output discrete-time model of a system in state-space format:

$$\boldsymbol{x}(k+1) = A\boldsymbol{x}(k) + B\boldsymbol{u}(k), \qquad \boldsymbol{y}(k) = C\boldsymbol{x}(k) + D\boldsymbol{u}(k) \tag{4}$$

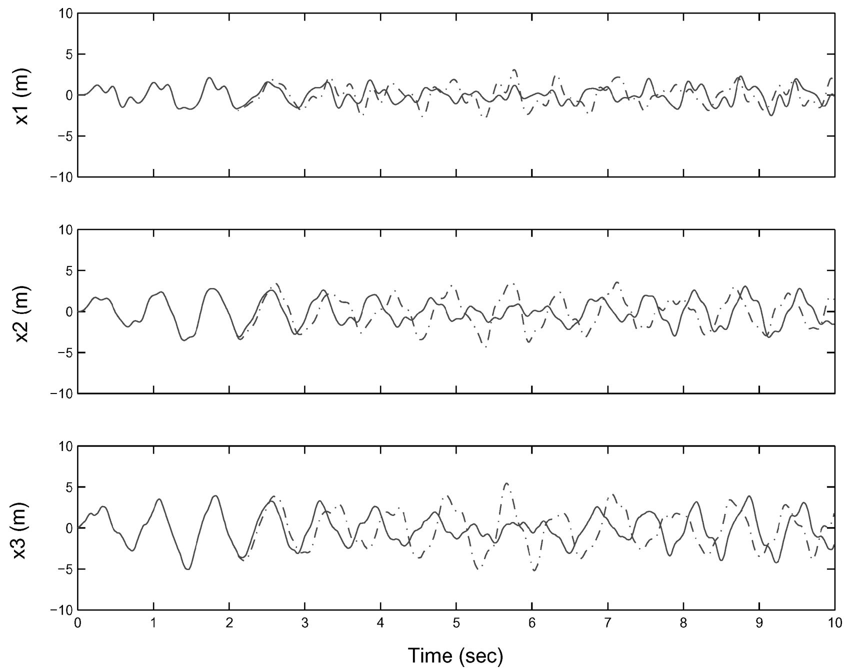

Fig. 2 Simulated time histories of displacement for the healthy and damaged spring–mass system: ——, healthy and ·—·, damaged.

By repeated substitution for some $p \geq 0$,

$$\boldsymbol{x}(k+p) = A^p \boldsymbol{x}(k) + \boldsymbol{C}\boldsymbol{u}_p(k), \qquad \boldsymbol{y}_p(k) = O\boldsymbol{x}(k) + T\boldsymbol{u}_p(k) \tag{5}$$

where $\boldsymbol{y}_p(k)$ and $\boldsymbol{u}_p(k)$ are defined as column vectors of input and output data going p steps into the future starting with $\boldsymbol{y}(k)$ and $\boldsymbol{u}(k)$, respectively,

$$\boldsymbol{y}_p(k) = \begin{bmatrix} \boldsymbol{y}(k) \\ \boldsymbol{y}(k+1) \\ \vdots \\ \boldsymbol{y}(k+p-1) \end{bmatrix}, \qquad \boldsymbol{u}_p(k) = \begin{bmatrix} \boldsymbol{u}(k) \\ \boldsymbol{u}(k+1) \\ \vdots \\ \boldsymbol{u}(k+p-1) \end{bmatrix} \tag{6}$$

For sufficiently large p, $\boldsymbol{C}$ is an extended $n \times pr$ controllability matrix, O is an extended $pm \times n$ observability matrix, and T is a $pm \times pr$ Toeplitz matrix of the system of Markov parameters:

$$\boldsymbol{C} = [A^{p-1}B, \ldots, AB, B], \qquad O = [C, CA, \ldots, CA^{p-1}]^T$$

$$T = \begin{bmatrix} D & 0 & 0 & \cdots & 0 \\ CB & D & \cdots & \cdots & 0 \\ CAB & CB & D & \cdots & \vdots \\ \vdots & \vdots & \vdots & \vdots & 0 \\ CA^{p-2}B & \cdots & CAB & CB & D \end{bmatrix} \tag{7}$$

Rewriting Eq. (5) in terms of contribution of each individual input $i = 1, 2, \ldots, r$,

$$\boldsymbol{x}(k+p) = A^p\boldsymbol{x}(k) + \boldsymbol{C}_1\boldsymbol{u}_1^{(p)}(k) + \cdots + \boldsymbol{C}_r\boldsymbol{u}_r^{(p)}(k) + \boldsymbol{B}_1\boldsymbol{u}_1(k+p-1) + \cdots + \boldsymbol{B}_r\boldsymbol{u}_r(k+p-1)$$

$$\boldsymbol{y}_p(k) = O\boldsymbol{x}(k) + T_1\boldsymbol{u}_1^{(p)}(k) + \cdots + T_r\boldsymbol{u}_r^{(p)}(k) + D_1\boldsymbol{u}_1(k+p-1) + \cdots + D_r\boldsymbol{u}_r(k+p-1) \tag{8}$$

where $B = [\boldsymbol{B}_1, \boldsymbol{B}_2, \ldots, \boldsymbol{B}_r]$ and $\boldsymbol{C}_i = [A^{p-1}\boldsymbol{B}_i, \ldots, A^2\boldsymbol{B}_i, A\boldsymbol{B}_i]$. Also,

$$\boldsymbol{u}_i^{(p)}(k) = \begin{bmatrix} \boldsymbol{u}_i(k) \\ \boldsymbol{u}_i(k+1) \\ \vdots \\ \boldsymbol{u}_i(k+p-2) \end{bmatrix}$$

$$T_i = \begin{bmatrix} D_i & 0 & \cdots & 0 \\ C\boldsymbol{B}_i & D_i & \ddots & \vdots \\ CA\boldsymbol{B}_i & C\boldsymbol{B}_i & D_i & \vdots \\ \vdots & \ddots & \ddots & D_i \\ CA^{p-2}\boldsymbol{B}_i & \cdots & CA\boldsymbol{B}_i & C\boldsymbol{B}_i \end{bmatrix} \tag{9}$$

An interaction matrix M_i is introduced by adding and subtracting the product $M_i\boldsymbol{y}_p(k)$ to Eq. (8). If the measurements are the position, the D matrix becomes a null matrix. It is easy to modify the same formulation to accommodate acceleration measurements[28]:

$$\begin{aligned} \boldsymbol{x}(k+p) &= A^p\boldsymbol{x}(k) + \boldsymbol{C}_1\boldsymbol{u}_1^{(p)}(k) + \cdots + \boldsymbol{C}_r\boldsymbol{u}_r^{(p)}(k) \\ &\quad + \boldsymbol{B}_1\boldsymbol{u}_1(k+p-1) + \cdots + \boldsymbol{B}_r\boldsymbol{u}_r(k+p-1) \\ &\quad + M_i\boldsymbol{y}_p(k) - M_i\boldsymbol{y}_p(k) \\ &= \left(A^p + M_iO\right)\boldsymbol{x}(k) + (\boldsymbol{C}_1 + M_iT_1)\boldsymbol{u}_1^{(p)}(k) \\ &\quad + \cdots + (\boldsymbol{C}_r + M_iT_r)\boldsymbol{u}_r^{(p)}(k) + \boldsymbol{B}_1\boldsymbol{u}_1(k+p-1) \\ &\quad + \cdots + \boldsymbol{B}_r\boldsymbol{u}_r(k+p-1) - M_i\boldsymbol{y}_p(k) \end{aligned} \tag{10}$$

Premultiplying Eq. (10) by C yields

$$\begin{aligned} \boldsymbol{y}(k+p) &= (CA^p + CM_iO)\boldsymbol{x}(k) + (C\boldsymbol{C}_1 + CM_iT_i)\boldsymbol{u}_1^{(p)}(k) \\ &\quad + \cdots + (C\boldsymbol{C}_r + CM_iT_r)\boldsymbol{u}_r^{(p)}(k) + C\boldsymbol{B}_1\boldsymbol{u}_1(k+p-1) \\ &\quad + \cdots + C\boldsymbol{B}_r\boldsymbol{u}_r(k+p-1) - CM_i\boldsymbol{y}_p(k) \end{aligned} \tag{11}$$

For each input i, impose conditions in Eq. (11) for the product CM_i in Eq. (10) so that coefficients of state $\boldsymbol{x}(k)$ terms and input vectors $\boldsymbol{u}_i^{(p)}(k)$ vanish identically except for that input:

$$CA^P + CM_iO = 0, \qquad C\boldsymbol{C}_j + CM_iT_j = 0, \qquad \forall j \neq i \tag{12}$$

The conditions for the existence of the product CM_i (which implied the existence of M_i for independent outputs) is satisfied if the number of independent sensors is at least equal to the number of members in the structure ($m \geq r$) so that failures among each actuators can be distinguished.

For each input i, we have

$$\boldsymbol{y}(k+p) = (C\boldsymbol{C}_i + CM_iT_i)\boldsymbol{u}_i^{(p)}(k) + C\boldsymbol{B}_1\boldsymbol{u}_1(k+p-1) + \cdots + C\boldsymbol{B}_r\boldsymbol{u}_r(k+p-1) - CM_i\boldsymbol{y}_p(k) \quad (13)$$

To monitor the integrity of the ith actuator, the relationship between the input and output should be established for each actuator. Specifically, certain input–output functions should generate error signals if and only if the ith actuator has failed. Premultiplying Eq. (13) with a row vector that is orthogonal to all remaining column vectors CB_j, $j \neq i$,

$$\boldsymbol{N}_i^T(CB_j) = 0, \qquad \forall j \neq i \quad (14)$$

Because $m \geq r$, such a vector $\boldsymbol{N}_i$ can be easily found. Premultiplying Eq. (13) by $\boldsymbol{N}_i$ produces a scalar equation that involves all measured outputs and ith input alone:

$$\boldsymbol{N}_i^T\boldsymbol{y}(k+p) = \boldsymbol{N}_i^T(C\boldsymbol{C}_i + CM_iT_i)\boldsymbol{u}_i^{(p)}(k) + \boldsymbol{N}_i^TC\boldsymbol{B}_i\boldsymbol{u}_i(k+p-1) - \boldsymbol{N}_i^TCM_i\boldsymbol{y}_p(k) \quad (15)$$

For each input i, when an error is defined and the time index is shifted back by p,

$$e_i(k) = \boldsymbol{N}_i^T\boldsymbol{y}(k) + \boldsymbol{N}_i^TCM_i\boldsymbol{y}_p(k-p) - \boldsymbol{N}_i^T(C\boldsymbol{C}_i + CM_iT_i) \times \bar{\boldsymbol{u}}_i^{(p)}(k-p) - \boldsymbol{N}_i^TC\boldsymbol{B}_i\bar{\boldsymbol{u}}_i(k-1) \quad (16)$$

where $\bar{\boldsymbol{u}}_i(k)$ is the commanded input such that $\boldsymbol{u}_i(k) = \bar{\boldsymbol{u}}_i(k) + z_i(\boldsymbol{k})$ where $z_i(\boldsymbol{k})$ is the actuator error.

Equation (16) assumes the general form

$$e_i(k) = \boldsymbol{\alpha}_0\boldsymbol{y}(k) + \boldsymbol{\alpha}_1\boldsymbol{y}(k-1) + \cdots + \boldsymbol{\alpha}_p\boldsymbol{y}(k-p) + \beta_1\bar{\boldsymbol{u}}_i(k-1) + \beta_2\bar{\boldsymbol{u}}_i(k-2) + \cdots + \beta_p\bar{\boldsymbol{u}}_i(k-p) \quad (17)$$

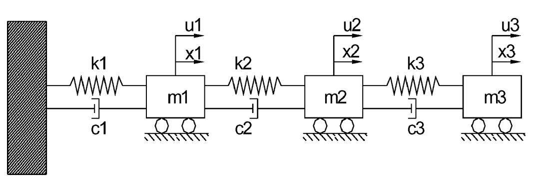

Fig. 3 Three-input (u_1, u_2, and u_3) and three-output (x_1, x_2, and x_3) spring–mass–damper system.

For an r-input/m-output system ($m \geq r$), each coefficient $\boldsymbol{\alpha}_0$, $\boldsymbol{\alpha}_1, \ldots, \boldsymbol{\alpha}_p$ is a $1 \times m$ row vector, whereas each coefficient β_1, $\beta_2, \ldots, \beta_p$ is a scalar. For the ith actuator, these coefficients are related to those of the original state-space model by

$$[\boldsymbol{\alpha}_p, \boldsymbol{\alpha}_{p-1}, \ldots, \boldsymbol{\alpha}_1, \boldsymbol{\alpha}_0] = \left[\boldsymbol{N}_i^TCM_i, \boldsymbol{N}_i^T\right]$$

$$[\beta_p, \beta_{p-1}, \ldots, \beta_2, \beta_1] = -\left[\boldsymbol{N}_i^T(C\boldsymbol{C}_i + CM_iT_i), \boldsymbol{N}_i^TC\boldsymbol{B}_i\right] \quad (18)$$

Given a state-space model of the healthy structure, the coefficients of Eq. (17) can be easily obtained from the calculation of the product CM_i and normalization vector $\boldsymbol{N}_i$. For structural damage monitoring, the nonzero error signal from Eq. (17) for the ith actuator indicates the initiation of structural damage at the ith stiffness member. Note that the number of outputs should be equal or greater than that of actuators to have a valid input error function as shown in Eq. (17).

C. Three-DOF Spring–Mass System

With the input error function developed, the next step is inferring the equivalence of stiffness damage in a structure from the internal force error. The elemental stiffness matrix of each structural member is coupled with neighboring DOF, which makes it difficult to derive a direct connection between input error function and damage-induced elemental stiffness residual forces. To get around this problem, the input influence matrix B_f has been properly modified. For the system shown in Fig. 1, the input influence matrix B_f and the input vector are

$$B_f = \begin{bmatrix} 1 & 0 & 0 \\ 0 & 1 & 0 \\ 0 & 0 & 1 \end{bmatrix}, \qquad \boldsymbol{u}(t) = \begin{bmatrix} u_1(t) \\ u_2(t) \\ u_3(t) \end{bmatrix} \quad (19)$$

Because there is no restriction on the choice of input combinations, we use the following:

$$\hat{B}_f = \begin{bmatrix} 1 & -1 & 0 \\ 0 & 1 & -1 \\ 0 & 0 & 1 \end{bmatrix}, \qquad \hat{\boldsymbol{u}}(t) = \begin{bmatrix} u_1(t) + u_2(t) + u_3(t) \\ u_2(t) + u_3(t) \\ u_3(t) \end{bmatrix} \quad (20)$$

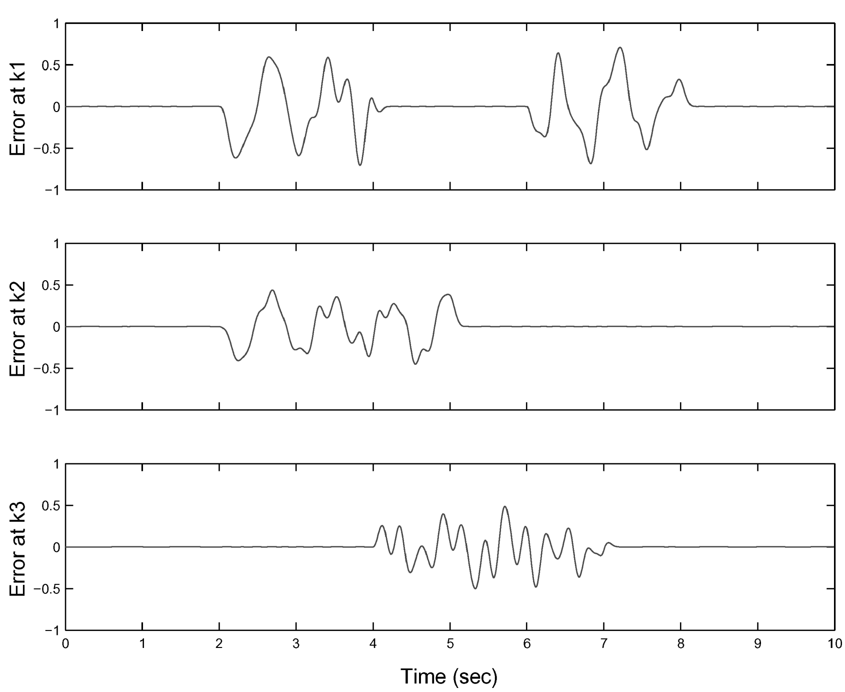

Fig. 4 Each input error function of the damaged spring–mass–damper system.

By modifying B_f as well as the input matrix, one can obtain the equivalent system, giving the same input–output relationship as

$$B_f \boldsymbol{u}(t) = \hat{B}_f \hat{\boldsymbol{u}}(t) \tag{21}$$

Accordingly, the dynamic equation of the damaged structure in Eq. (3) becomes

$$M\ddot{\boldsymbol{q}}(t) + \Theta\dot{\boldsymbol{q}}(t) + K\boldsymbol{q}(t) = \hat{B}_f \hat{\boldsymbol{u}}(t) + \Delta \boldsymbol{u}(t) \tag{22}$$

This transformation will eliminate the coupled error signal due to damages in neighboring structural members, while representing the same input system. Hence, each input error function will be able to monitor the occurrence of damage for a specific structural member. The original B_f matrix represents a system where actuators are embedded between a DOF and fixed ground (external actuators), whereas the modified $\hat{B}_f$ matrix represents a system where internal actuators are embedded between DOF, like springs in this case. Here, the modified input influence matrix $\hat{B}_f$ represents a system having internal or virtual actuators. These virtual actuators will produce a nonzero error signal when the stiffness of the spring changes. If we use this virtual input system, it is possible to obtain a unique error function that corresponds to a specific spring in the system. This concept is demonstrated by following numerical simulations.

Consider a three-DOF spring–mass–damper system (Fig. 3) where stiffness of spring 1, k_1, and spring 2, k_2, is subject to change after 2 s. The stiffness of spring 3, k_3, is supposed to change after 4 s. This simulation is an example of simultaneously occurring multiple stiffness damages in a structure. Here, two physical actuators excite the second and third masses (m_2 and m_3), while three virtual actuators are implicitly implanted at all DOF. The error function corresponding to each spring is shown in Fig. 4. It is clear that the initiation of damage in springs 1 and 2 can be easily determined from 2 s onward. The error function of spring 3 also illustrates the correct profile of the stiffness changes. The profile of the error function is similar to the parity check that can be used to capture the failure of the system.[14] Although the input error function is originally developed for detecting actuator failure,[28] the equivalence between the stiffness damage and input error can justify its application for solving real-time damage monitoring problems. From the comparison of Figs. 2 and 4, we see that influences of all other damages in different time instants and locations are clearly decoupled from a specific damage that is being examined. Hence, it can be concluded that real-time damage monitoring is possible through the actuator failure detection algorithm.

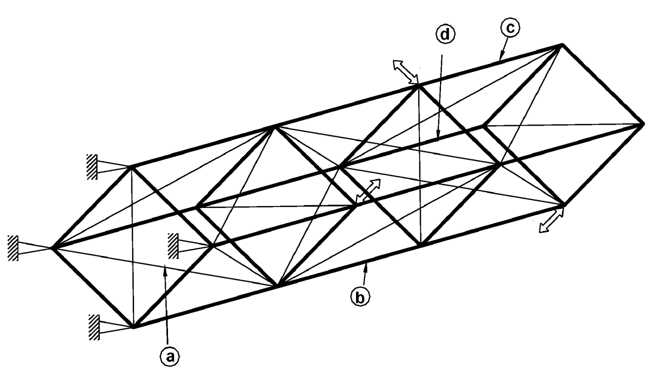

Fig. 5 Schematic of three-bay cantilevered truss structure.

III. Numerical Simulation for Real-Time Damage Monitoring: Three-Dimensional Truss Structure

Consider an analytical model of a three-dimensional aluminum truss structure (Fig. 5) to validate the aforementioned damage monitoring method. This three-bay truss model consists of 44 rod elements connected at 36 nodes. A schematic diagram of the structure, along with the locations and the directions of excitation inputs (arrows), is shown in Fig. 5. The total length of the truss is 1.5 m, and each bay has 0.5-m-long battens. All of the members, battens, and longerons are hollow tubes with outer diameter equal to 0.0127 m, thickness of 0.00254 m, and Young's modulus of $E = 6.89 \times 10^9$ N/m^2. Here, proportional damping is considered as $\Theta = aK + bM$, where a and b are constants. The response of position at each DOF is simulated for damage monitoring. Random noise input forces are applied to the structure. The first four modal frequencies of the three-bay three-dimensional truss structure are determined as 19.66, 22.85, 34.80, and 65.78 Hz, respectively. In this simulation, only four members (a–d) of the total 44 members are considered to be damaged, as shown in Fig. 5.

Because this study concerns real-time damage monitoring, multiple stiffness damages are purposely imposed on certain members of the structure at some unknown time instant and at unknown location, as shown in Fig. 6. Although it is very unlikely that a damage, once it occurred in the structure, can be fully recovered after some time interval, the intermittent stiffness variation is simulated to emphasize the on-line monitoring capability of the method. Specifically, sequences of stiffness damage for each truss member are shown in Fig. 6. A more practical damage scenario is considered in one of the truss members. In member a, it is assumed that after 20 s joint failure has occurred, which is similar to the situation of a breathing crack. Thus, if damage occurs in member a, its stiffness alternately changes from 100% in compression mode to 10% in tension mode as shown in Fig. 6b. Figure 7 shows the profile of the error function $e_i(k)$ of the damaged truss members. In Fig. 7, zero and nonzero error signals are clearly distinguished among the healthy, damaged, and recovered states of each member, showing successful real-time damage monitoring. The simulation result shows that given desired

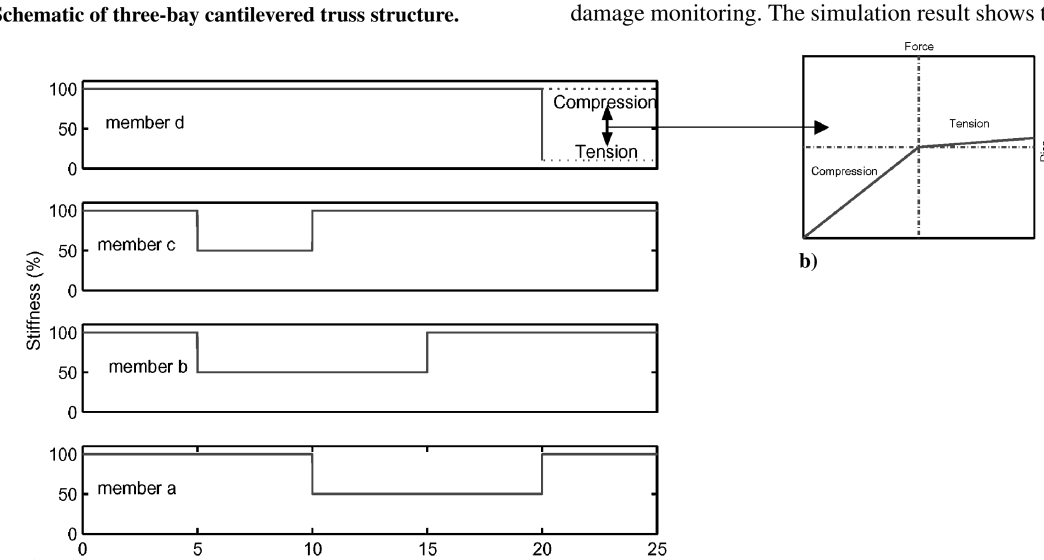

Fig. 6 Stiffness transition in members a–d.

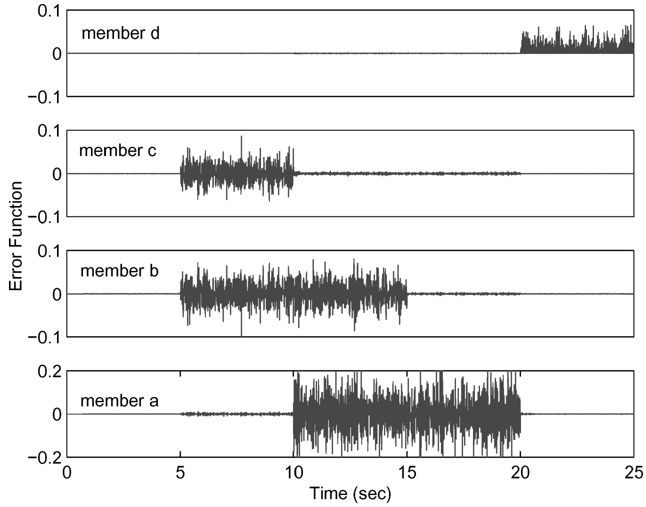

Fig. 7 Error functions corresponding to members of truss structure.

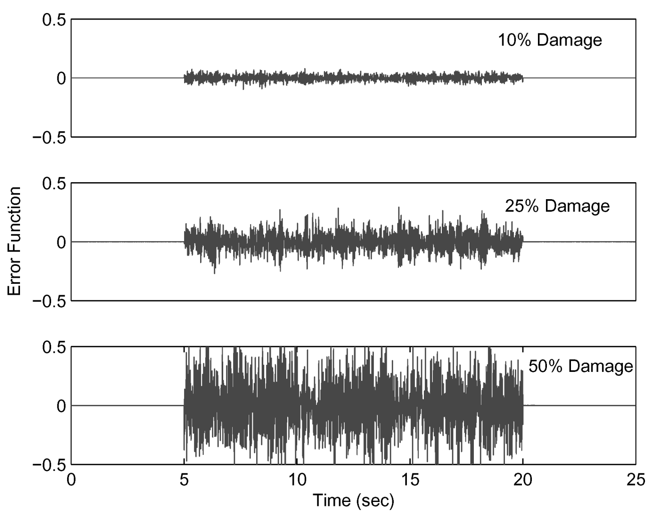

Fig. 8 Error functions of three different damage levels 10, 25, and 50% in truss member c.

(commanded) inputs and analytical model of the structure damages can be individually detected and isolated from input error signals regardless of numbers, time instants, and locations of damages. Also, note that it is possible to distinguish the nature of damage to some extent. Whereas error functions corresponding to the members having open-crack-type damages (members b–d) are symmetric, the error function corresponding to the bilinear breathing damage (member a) is not. Note that a damage type having a directional bias can be identified from the unsymmetrical profile of error signal.

In a strict sense, this particular technique belongs to model-based damage detection methods which resort to an analytical redundancy. One significant benefit of the proposed method is that parameters $\boldsymbol{\alpha}_i$ and β_i in error function $e_i(k)$ of Eq. (17) can be derived from the experimentally identified state-space model, which is the baseline model of the healthy structure. Moreover, $\boldsymbol{\alpha}_i$ and β_i can be also directly obtained from the input–output data, bypassing the process of state-space model identification in a certain class of systems. For practical application of this method, previously recorded input–output data from the undamaged structure can be used to monitor the occurrence of future damage of the same structure. For a feasibility study of damage monitoring, the percentage of stiffness loss at each truss member is chosen as a damage parameter. Note that the mass of each damaged member is assumed to be unchanged. However, the same formulation can be applied for the detection of mass changes in the structure. Although the error signal does not have a physical meaning or interpretation per se, it is obvious that the level of the error signal is proportional to the intensity of the stiffness damage. Figure 8 shows three different damage levels, 10, 25, and 50% of stiffness reduction for member c between 5 and 20 s and the corresponding amplitude of error functions. Apparently, the larger the error signal is, the more severe is the structural damage. Thus, the extent of specific damage can be approximated by observing the deviation of the error signal using some statistical measures.

IV. Conclusions

This paper introduces and demonstrates the performance of newly developed real-time damage monitoring technique. A real-time approach provides an alternative to the modal-based diagnosis method. Because the method directly uses time-domain measurements, it readily works for nonlinear damage models. The presented method needs any type of command input, analytical model of the healthy structure, and time-domain responses of the potentially damaged structure. The theory is based on input error functions developed from the modified formulation of the interaction matrix. Specifically, the method exploits the analogy between local stiffness damage in a structure and the actuator failure problem. The stiffness damage or internal force error can be isolated via a special error function, where the influence of erroneous inputs to the system can be completely decoupled from the outputs. Thus, the presence of stiffness damage in each structural member can be inferred by observing the residual signal. This input error function is successfully used for real-time monitoring of structural damages, demonstrated by numerical simulation of a three-dimensional truss structure.

Acknowledgment

The authors acknowledge the support of the Texas Institute for the Intelligent Bio-Nano Materials and Structure for Aerospace Vehicles, funded by NASA Cooperative Agreement NCC-1-02038.

References

[1]Zou, Y., Tong, L., and Steven, G. P., "Vibration-Based Model-Dependent Damage (Delamination) Identification and Health Monitoring for Composite Structure—A Review," *Journal of Sound and Vibration*, Vol. 230, No. 2, 2000, pp. 357–378.

[2]Cawley, P., and Adams, R. D., "The Location of Defects in Structures from Measurements of Natural Frequencies," *Journal of Strain Analysis*, Vol. 14, No. 2, 1979, pp. 49–57.

[3]Contursi, T., Mangialardi, L. M., and Messina, A., "Structural Damage Detection by Sensitivity and Statistical-Based Method," *Journal of Sound and Vibration*, Vol. 216, No. 5, 1998, pp. 791–808.

[4]Agneni, A., Balis Crema, L., and Mastroddi, F., "Damage Detection from Truncated Frequency Response Functions," *European COST F3 Conference on System Identification and Structural Health Monitoring*, Madrid, 2000, pp. 137–146.

[5]Kaouk, M., and Zimmerman, D. C., "Structural Damage Assessment Using a Generalized Minimum Rank Perturbation Theory," *AIAA Journal*, Vol. 32, No. 4, 1994, pp. 836–842.

[6]Schulz, M. J., Pai, P. F., and Abdelnaser, A. S., "Frequency Response Function Assignment Technique for Structural Damage Identification," *Proceedings of 14th International Modal Analysis Conference*, Dearborn, MI, 1996, pp. 105–111.

[7]Tasker, F., Dunn, B., and Fisher, S., "Online Structural Damage Detection Using Subspace Estimation," *Proceedings of the 1999 IEEE Aerospace Conference* [CD-ROM], Track 3, Paper 3.402, Aspen, CO, 1999.

[8]Cattarius, J., and Inman, D. J., "Time Domain Analysis for Damage Detection in Smart Structures," *Mechanical Systems and Signal Processing*, Vol. 11, No. 3, 1997, pp. 409–423.

[9]Carneiro, S. H. S., "Model-Based Vibration Diagnostic of Cracked Beams in the Time Domain," Ph.D. Dissertation, Dept. of Engineering Science and Mechanics, Virginia Polytechnic Inst. and State Univ., Blacksburg, VA, Aug. 2000.

[10]Banks, H. T., Inman, D. J., Leo, D. J., and Wang, Y., "An Experimentally Validated Damage Detection Theory in Smart Structures," *Journal of Sound and Vibration*, Vol. 191, No. 5, 1996, pp. 859–880.

[11]Clark, R. N., Fosth, D. C., and Walton, V. M., "Detecting Instrument Malfunctions in Control Systems," *IEEE Transactions on Aerospace and Electronic Systems*, Vol. AES-11, No. 4, 1975, pp. 465–473.

[12]Chen, J., and Patton, R. J., *Robust Model-Based Fault Diagnosis for Dynamic Systems*, Kluwer Academic, 1998.

[13]Chow, E. Y., and Willsky, A. S., "Analytical Redundancy and the Design of Robust Failure Detection Systems," *IEEE Transactions on Automatic Control*, Vol. 29, No. 7, 1984, pp. 603–614.

[14]Frank, P. M., "Fault Diagnosis in Dynamic Systems Using Analytical and Knowledge-Based Redundancy—A Survey and Some New Results," *Automatica*, Vol. 26, No. 3, 1990, pp. 459–474.

[15]Osder, S., "Practical View of Redundancy Management Application and Theory," *Journal of Guidance, Control, and Dynamics*, Vol. 22, No. 1, 1999, pp. 12–21.

[16]Kranock, S. J., "Real-Time Structural Damage Detection Using Model-Based Observers," Ph.D. Dissertation, Dept. of Aerospace Engineering Science, Univ. of Colorado, Boulder, CO, Feb. 2000.

[17]Seibold, S., and Weinert, K., "A Time Domain Method for the Localization of Cracks in Rotors," *Journal of Sound and Vibration*, Vol. 195, No. 1, 1996, pp. 57–73.

[18]Demetriou, M. A., and Hou, Z., "On-Line Fault/Damage Detection Schemes for Mechanical and Structural Systems," *Journal of Structural Control*, Vol. 10, No. 1, 2003, pp. 1–23.

[19]Chati, M., Rand, R., and Mukherjee, S., "Modal Analysis of a Cracked Beam," *Journal of Sound and Vibration*, Vol. 207, No. 2, 1997, pp. 249–270.

[20]Cheng, S. M., Wu, X. J., Wallace, W., and Swamidas, A. S. J., "Vibrational Response of a Beam with a Breathing Crack," *Journal of Sound and Vibration*, Vol. 225, No. 1, 1999, pp. 201–208.

[21]Chondros, T. G., Dimarogonas, A. D., and Yao, J., "Vibration of a Beam with a Breathing Crack," *Journal of Sound and Vibration*, Vol. 239, No. 1, 2001, pp. 57–67.

[22]Leonard, F., Lanteigne, J., Lalonde, S., and Turcotte, Y., "Free-Vibration Behavior of a Cracked Cantilever Beam and Crack Detection," *Mechanical Systems and Signal Processing*, Vol. 15, No. 3, 2001, pp. 529–548.

[23]Phan, M. Q., Lim, R. K., and Longman, R. W., "Unifying Input–Output and State-Space Perspectives of Predictive Control," Dept. of Mechanical and Aerospace Engineering, Technical Rept. 3044, Princeton Univ., Princeton, NJ, Sept. 1998.

[24]Lim, R. K., Phan, M. Q., and Longman, R. W., "State Estimation with ARMarkov Models," Dept. of Mechanical and Aerospace Engineering, Technical Rept. 3046, Princeton Univ., Princeton, NJ, Oct. 1998.

[25]Goodzeit, N. E., and Phan, M. Q., "System Identification in the Presence of Completely Unknown Periodic Disturbances," *Journal of Guidance, Control, and Dynamics*, Vol. 23, No. 2, 2000, pp. 251–259.

[26]Darling, R. S., and Phan, M. Q., "Dynamic Output Feedback Predictive Controllers for Vibration Suppression and Periodic Disturbance Rejection," AAS Paper 04-0154, Feb. 2004.

[27]Darling, R. S., and Phan, M. Q., "Predictive Controllers for Simultaneous Tracking and Disturbance Rejection," AIAA Paper 2004-5109, Aug. 2004.

[28]Koh, B. H., Li, Z., Dharap, P., Nagarajaiah, S., and Phan, M. Q., "Actuator Failure Detection Through Interaction Matrix Formulation," *Journal of Guidance, Control and Dynamics* (to be published).

A. Palazotto
Associate Editor